Magnetic susceptibility measurements of polycrystalline samples between 84 and 295 K strictly obey the Curie–Weiss law of the form (1), where $Ng^2\beta^2/4k = C$, $\chi_M$ is the molar susceptibility

$$\chi_M = \frac{Ng^2\beta^2}{4k(T-\Theta)} + N\alpha \qquad (1)$$

corrected for diamagnetism ($-716.6 \times 10^{-6}$ cgsu), $N\alpha$ is the temperature-independent paramagnetism (TIP = $120 \times 10^{-6}$ cgsu for the dimer molecule).

A least-squares fit of the reciprocal of molar susceptibility, corrected for both the diamagnetism and temperature-independent paramagnetism, vs. temperature according to the equation (1) gives a $C$ value of 2.271 cgsu, $\Theta$ = 7.2 K, and $g$ = 2.16 in agreement with the average value of 2.15 obtained from EPR spectra (Table IV). The EPR spectra at different temperatures (4, 139, 298 K) are very similar to one another, are of the axial type, and show a sharp maximum in the 3000-G spectral region, while a further low-field resonance corresponding to $\Delta M_s = 2$ is present in the spectrum at 139 K (Figure 2). This transition indicates the presence of magnetically coupled copper(II) ions within each dimer,[24] but the very good agreement of magnetic data down to 84 K with eq 1 suggests that exchange interactions allow only for a very small $|2J|$ value, in agreement with the reported value for the structurally analoguous $[Cu(Hippu)_2(H_2O)_4]_2$ ($|2J|$ = 4.3 $cm^{-1}$ [25]), attributable to the quasi-orthogonality between the s and p orbitals on the bridging oxygen and the orbital on one copper that contains the unpaired spin (Cu–O–Cu = 100.0 (1)° in the present complex and 101.0° in the hippurato complex).

The EPR and electronic parameters (Table IV) are similar to those of square-pyramidal copper(II) complexes with the $CuN_2O_3$ chromophore,[26] and comparison with the spectroscopic data of $[Cu(Hippu)_2(H_2O)_4]_2$ (d–d band maxima: 680 and 880 nm,[20] 685 and 900 sh nm,[27] $g_\parallel$ = 2.356 and $g_\perp$ = 2.068[28]) reveals the expected displacement of d–d band maxima to greater energy and that of $g$ parameters to lower values because of the chromophore change from $CuO_5$ in the hippurate derivative to $CuN_2O_3$ in tosylglycinate.

In the infrared spectrum (Table IV), the absorption frequencies of the uncoordinated functional groups (NH, $SO_2$) are in the range found for the other copper(II)–*N*-tosylglycinate monoanion complexes[4] and for $[Cu(Ts\text{-}\beta\text{-}AlaH)_2(bpy)]$[7] except for the polymeric $[Cu(TsGlyH)_2]_n$, which shows one sulfonic oxygen coordinated to the copper atom[4c]). The only significant difference among the infrared spectra of the present and of previously cited complexes concerns the splitting of the absorption frequencis of the carboxylate group as a consequence of the different bonding modes in which this group is involved in the present complex. The asymmetric stretching band at 1650 $cm^{-1}$ is assigned to the bridging carboxyl group and that at 1600 $cm^{-1}$ to the monodentate carboxyl group; a broad unresolved band assignable to the symmetric stretching of both carboxyl groups is found at 1370 $cm^{-1}$. In Table IV we also report the bands attributable to the water molecule.

**Acknowledgment.** The authors are grateful to the Centro di Calcolo Elettronico dell'Università di Modena for computing support, the Centro Strumenti dell'Università di Modena for recording the infrared spectra, Prof. A. Vacca of ISSECC, CNR, Florence, Italy, for allowing the use of EPR spectrometers, and Prof. G. C. Pellacani for helpful discussions.

**Registry No.** $[Cu(TsglyH)_2(bpy)]_2 \cdot 2H_2O$, 94203-47-1; $[Cu(TsglyH)_2(bpy)]_2 \cdot 4H_2O$, 94292-15-6.

**Supplementary Material Available:** Lists of observed and calculated structure factors, atomic temperature factors, hydrogen atom parameters, complete bond distances and bond angles, hydrogen bonding distances and angles, selected least-squares planes, and experimental and calculated corrected molar susceptibilities and magnetic moments (27 pages). Ordering information is given on any current masthead page.

(24) Villa, J. F.; Hatfield, W. E. *Inorg. Chem.* **1972**, *11*, 1331.
(25) Estes, E. D.; Estes, W. E.; Scaringe, R. P.; Hatfield, W. E.; Hodgson, D. J. *Inorg. Chem.* **1975**, *14*, 2564.
(26) Dehand, J.; Jordanov, J.; Keck, F.; Mosset, A.; Bonnet, J. J.; Galy, J. *Inorg. Chem.* **1979**, *18*, 1543.
(27) Marcotrigiano, G.; Pellacani, G. C. *Z. Anorg. Allg. Chem.* **1975**, *413*, 171.
(28) Gaura, R.; Kokoszka, G.; Hyde, K. E.; Lancione, R. *J. Coord. Chem.* **1976**, *5*, 105.

Contribution from the Department of Chemistry, Michigan State University, East Lansing, Michigan 48824

# Intercalation of Niobium and Tantalum $M_6Cl_{12}^{n+}$ Cluster Cations in Montmorillonite: A New Route to Pillared Clays

STEVEN P. CHRISTIANO, JIALIANG WANG, and THOMAS J. PINNAVAIA*

*Received July 9, 1984*

A new synthetic route to pillared clays is described that is based on the intercalation and subsequent oxidation of metal cluster cations in montmorillonite. Niobium and tantalum clusters of the type $M_6Cl_{12}^{n+}$ ($n$ = 2, 3) are shown to bind to the clay by ion exchange for interlayer sodium. The maximum cluster loading is larger than expected on the basis of formal cation charge and clay ion-exchange capacity, indicating that reduction of cluster charge occurs through hydrolysis on the intracrystal surfaces. The intercalated products exhibit regular basal spacings of 18.4 ± 0.2 Å (M = Nb) and 18.9 ± 0.5 Å (M = Ta). Oxidation of the intercalated cluster cations by water at 240 °C results in the in situ formation of metal oxide aggregates that function as molecular size pillars. The niobium and tantalum oxide pillared clays exhibit basal spacings of 19.9 ± 0.5 Å and are thermally stable to 400 °C.

## Introduction

Pillared clays are smectite clay minerals that have been modified through the introduction of robust cations into their interlayer regions. The intercalated cations function as molecular props or pillars between the silicate layers, creating a highly porous structure with a large intracrystalline surface area suitable for molecular absorption and catalysis. Early pillaring experiments by Barrer and co-workers[1,2] dealt with the intercalation of alkylammonium ions in montmorillonite. These bulky cations propped the silicate sheets apart by 4.0–4.5 Å and markedly improved the diffusive and sorbtive properties of the host silicate. Later work by Shabtai et al.[3] and by Berkheiser and Mortland[4] utilized the sterically rigid protonated dication of 1,4-diazabicyclo[2.2.2]octane to achieve an interlayer free spacing of approximately 5 Å. The alkylammonium pillared clays, however, were

(1) Barrer, R. M.; MacLeod, D. M. *Trans. Faraday Soc.* **1955**, *51*, 1290.
(2) Barrer, R. M.; Reay, J. S. S. *Trans. Faraday Soc.* **1957**, *53*, 1253.
(3) Shabtai, J.; Frydman, N.; Lazar, R. *Proc. 6th Int. Congr. Catal.* **1976**, *135*, 1.
(4) Mortland, M. M.; Berkheiser, V. *Clays Clay Miner.* **1976**, *24*, 60.

0020-1669/85/1324-1222$01.50/0 © 1985 American Chemical Society

stable in air to only moderate temperatures (approximately 250 °C). The intercalation of the metal chelate cations $M(chel)_3^{2+}$ (M = Fe, Ni; chel = phen, bpy) by Loeppert et al.[5] provided somewhat more stable pillared montmorillonites (approximately 350 °C) with an interlayer free spacing of approximately 8 Å.

The most thermally stable and thus most promising systems for catalytic purposes are those that utilize inorganic oxides as pillars. The intercalation of polynuclear oxycations of aluminum[6-9] and zirconium,[10] for instance, leads to alumina and zirconia pillared clays with interlayer free spacings of 6–10 Å and thermal stabilities in excess of 500 °C. Although the exchange reaction of smectite clays with polynuclear oxycations is an effective route to pillared clays, the method is severely limited by the aqueous solution chemistry of the metal ions used to form the pillars. An alternative and potentially more versatile route to pillared clays involve the use of metal complex cations as pillar precursors. The in situ conversion of an intercalated metal complex to a molecular size oxide aggregate should be applicable to a wide variety of metal ion systems that do not form stable polyoxycations in aqueous solution. The viability of such an approach was demonstrated by Endo et al.[11,12] in the synthesis of a silica-pillared montmorillonite via the hydrolysis of tris(acetylacetonato)silicon(IV) cations in the interlayer region. The silica-pillared clay possessed excellent thermal stability (>500 °C), but the interlayer free spacing was relatively low (approximately 3.0 Å). The magnitude of the interlayer free spacing was most likely limited by the amount of silicon that could be intercalated (1.0 Si per exchange equivalent of clay).

In the present study we examine the intercalation of niobium and tantalum cluster cations of the type $M_6Cl_{12}^{n+}$ ($n$ = 2, 3) in montmorillonite. These cluster cations exhibit a number of properties that make them attractive as precursors to metal oxide pillars. For instance, the hydrolysis and oxidation of the cations occur under relatively mild reaction conditions[13-15] so that the conversion to interlayer oxide aggregates should be quite facile. Also, the expected presence of 2.0–3.0 metal atoms per exchange equivalent should lead to interlayer free spacings that are larger than those found for silica pillared clays.

## Experimental Section

**$M_6Cl_{12}^{n+}$ Salts.** A mixed-valence chloride salt containing $Nb_6Cl_{12}^{n+}$ cluster cations was prepared by the reduction of niobium pentachloride with cadmium according to a previously described procedure.[16] Although efforts were made to obtain a pure salt with $n$ = 2 by minimizing air oxidation,[17,18] analysis of the final product by quantitative electron spin resonance spectroscopy,[19,20] together with UV–vis spectroscopy, indicated the presence of mixed-valence states with $n$ = 2 and 3 in approximately equal amounts. Nevertheless, the mixed-valence product proved to be useful for examining the mechanism of cluster binding.

The conproportionation of $NbCl_5$ and Nb in the presence of NaCl[17] was used to prepare $[Nb_6Cl_{12}]Cl_2 \cdot 8H_2O$ in good yield. UV–vis $\lambda_{max}$ ($H_2O$): 905, 405, 324, 275 nm. ESR indicated the presence of <10% $Nb_6Cl_{12}^{3+}$ ($g$ = 1.95 $\Delta H$ = 600 G).

$[Ta_6Cl_{12}]Cl_2 \cdot 9H_2O$ was prepared from $TaCl_5$ according to the method of Kuhn and McCarley.[21] The UV–vis spectrum gave $\lambda_{max}$ ($H_2O$) of 750, 635, 472, 395, 327, and 282 nm, in good agreement with the reported spectrum[21,22] for $Ta_6Cl_{12}^{2+}$. ESR spectroscopy ($g$ = 1.91) indicated the presence of some $Ta_6Cl_{12}^{3+}$.

**$Na^+$–Montmorillonite.** Natural Wyoming montmorillonite was obtained in spray-dried form from the Source Clay Repository, University of Missouri. The sample was suspended in water (1.0 wt %) and allowed to sediment 24 h to remove carbonate and other dense impurities. The suspended clay fraction was decanted, collected by centrifugation, and then resuspended in 1.0 N NaCl to ensure complete exchange to the $Na^+$ form. The clay was washed free of excess salt with distilled water and freeze-dried. Five independent analyses for $Na^+$, $Al^{3+}$, $Fe^{3+}$, $Mg^{2+}$, and $Si^{4+}$ gave the following anhydrous unit cell composition:

$$Na_{0.50}[Al_{3.11}Mg_{0.50}Fe_{0.40}](Si_{7.91}Al_{0.09})O_{20}(OH)_4$$

Analysis of the $Ni^{2+}$-saturated form of the clay indicated the cation-exchange capacity to be 60.2 mequiv/100 g of air-dried clay containing approximately 10 wt % $H_2O$, in agreement with the unit cell formula.

**$M_6Cl_{12}^{n+}$ Binding Curves.** The binding of $M_6Cl_{12}^{n+}$ cations to montmorillonite was studied spectrophotometrically. Each point on the binding curve was obtained by allowing the clay to equilibrate 18 h with a solution containing a known amount of cluster cation. The amount of cluster cation remaining in solution at equilibrium was determined by use of a standard absorbance curve constructed from solutions of known concentrations. The amount of cluster bound to the clay was then determined by difference. Emission spectroscopy was used to determine the amount of sodium released to solution upon cluster cation binding. Corrections were made for small amounts of $Na^+$ in the cluster stock solutions and in a montmorillonite blank suspension. All procedures were carried out while attempting to minimize contact with atmospheric oxygen.

**$M_2O_5$ Pillared Clays.** Montmorillonites pillared by molecular size aggregates of $M_2O_5$ were prepared by the in situ hydrolysis and oxidation of the intercalated $M_6Cl_{12}^{n+}$ cations. Intercalated montmorillonites containing 33 mmol of $Nb_6Cl_{12}^{2+}$ and 23 mmol of $Ta_6Cl_{12}^{2+}$ per 100 g of clay were subjected to heating under vacuum at 130 °C for 24 h followed by heating at 240 °C for 24 h. Elemental analysis indicated the presence of 1.19 Nb and 0.23 Cl per unit cell for the product pillared by niobium oxide and 0.98 Ta and 0.12 Cl per unit cell for the tantalum oxide pillared clay. The Nb and Ta contents of the final products are compatible with the initial cluster loadings, indicating that little or no metal complex is lost through sublimation in the thermolysis process.

**Chemical Analysis.** The elemental analyses used to derive the unit cell formula of $Na^+$–montmorillonite were determined by inductively coupled plasma emission spectroscopy on a Jarrell-Ash Model 955 Autocomp spectrophotometer. Samples were fused in $LiBO_2$ at 1000 °C, and the resulting glass was dissolved in dilute nitric acid. NBS standard clay 98a was used as a primary standard. The nickel cation-exchange capacity of the montmorillonite was determined by dissolving the $Ni^{2+}$-saturated clay in boiling $HCl/HNO_3$ and precipitating the $Ni^{2+}$ as the dimethylglyoxime complex. Niobium, tantalum, and chlorine analyses were performed by Galbraith Laboratory, Knoxville, TN.

**Physical Methods.** Nitrogen BET surface areas were determined with a Perkin-Elmer Model 212 B sorbtometer. Differential scanning calorimetry experiments were carried out on a Du Pont Model 990 thermal analyzer at a scan rate of 10°/min. X-ray diffraction data were collected by use of a Philips X-ray diffractometer with Ni-filtered Cu K$\alpha$ radiation; samples were thin films mounted on glass slides. XPS measurements were provided by Dr. Luis Matienzo, Martin-Marietta Corp., using a Physical Electronics Model 548 XPS-Auger spectrometer. The carbon 1s binding energy (284.6 eV) served as reference. UV–vis spectra were obtained on a Cary 17D or Cary 219 spectrophotometer; samples were mulled in Nujol and held between quartz glass plates. IR spectra of samples prepared in the form of KBr pellets were obtained on a Perkin-Elmer 457 spectrophotometer. ESR spectra were obtained for freeze-dried montmorillonite and solid cluster cation salts on a Varian E-4 spectrometer. For quantitative ESR measurements, the intensity of the first-derivative signal was calibrated against a $CuSO_4 \cdot 5H_2O$ reference sample by a numerical double-integration method.[19,20]

## Results

The reaction of $Nb_6Cl_{12}^{2+}$ and $Nb_6Cl_{12}^{3+}$ in 1:1 ratio, henceforth abbreviated $Nb_6Cl_{12}^{2+,3+}$, with $Na^+$–montmorillonite in aqueous suspension produces a green clay complex. A plot of the amount of cluster cation bound vs. the equilibrium concentration of


(5) Loeppert, R. H.; Mortland, M. M.; Pinnavaia, T. J. *Clays Clay Miner.* **1979**, *27*, 201.
(6) Lahav, N.; Shani, U.; Shabtai, J. *Clays Clay Miner.* **1978**, *26*, 107.
(7) Brindley, G. W.; Samples, R. E. *Clay Miner.* **1977**, *12*, 229.
(8) Lussier, R. J.; Magee, J. S.; Vaughan, D. E. W. *Preprints, 7th Canadian Symposium Catalysis* Edmonton, Alberta, **180**; pp 88–95.
(9) Occelli, M. L.; Tindwa, R. M. *Clays Clay Miner.* **1983**, *31*, 22.
(10) Yamanaka, S.; Brindley, G. W. *Clays Clay Miner.* **1979**, *27*, 119.
(11) Endo, T.; Mortland, M. M.; Pinnavaia, T. J. *Clays Clay Miner.* **1980**, *28*, 105.
(12) Endo, T.; Mortland, M. M.; Pinnavaia, T. J. *Clays Clay Miner.* **1981**, *29*, 153.
(13) Allen, R. J.; Sheldon, J. C. *Austr. J. Chem.* **1965**, *18*, 277.
(14) Brnicevic, N.; Shafer, H. *Z. Anorg. Allg. Chem.* **1978**, *441*, 219.
(15) Hughes, R. G.; Mayer, J. L.; Fleming, P. B.; McCarley, R. E. *Inorg. Chem.* **1970**, *9*, 1343.
(16) Harned, H. S.; Pauling, C.; Corey, R. B. *J. Am. Chem. Soc.* **1960**, *82*, 4815.
(17) Koknat, F. W.; Parsons, J. A.; Vongvvsharintra, A. *Inorg. Chem.* **1974**, *13*, 1699.
(18) Fleming, P. B.; Meyer, J. L.; Grindstaff, W. K.; McCarley, R. E. *Inorg. Chem.* **1970**, *9*, 1769.
(19) Aasa, R.; Vanngard, T. *J. Magn. Reson.* **1975**, *19*, 308.
(20) Ayscough, P. B. "Electron Spin Resonance in Chemistry"; Methuen: London, 1962; Appendix 5.
(21) Kuhn, P. J.; McCarley, R. E. *Inorg. Chem.* **1965**, *4*, 1482.

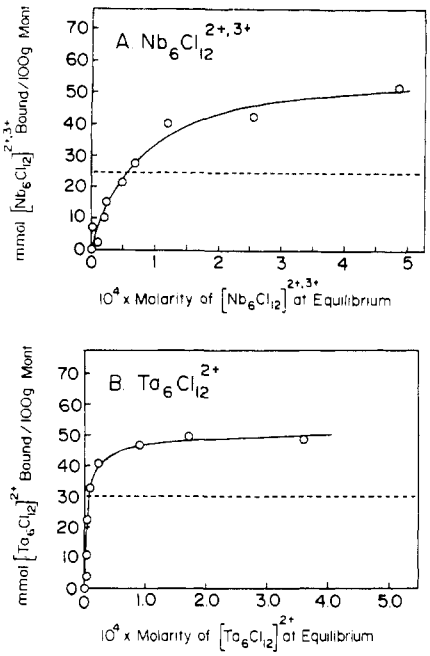


**Figure 1.** Binding at 25 °C of (A) $Nb_6Cl_{12}^{2+,3+}$ and (B) $Ta_6Cl_{12}^{2+}$ by $Na^+$–montmorillonite. The dashed lines indicate the binding limits expected for the displacement of 60 mequiv of $Na^+$/100 g of clay by cluster cations with the formal charges shown.

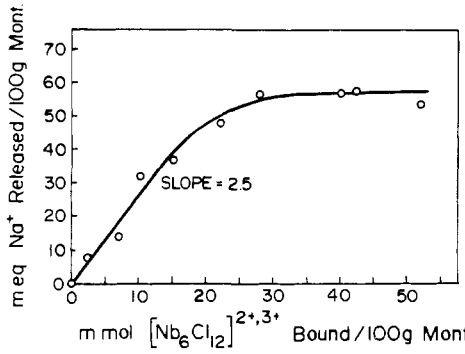


**Figure 2.** Relationship between the $Na^+$ released and the $Nb_6Cl_{12}^{2+,3+}$ bound by $Na^+$–montmorillonite.

$Nb_6Cl_{12}^{2+,3+}$ is shown in Figure 1A. The appreciable affinity of the cluster cations for the clay surface is indicated by the initial slope of the binding curve and the relatively low equilibrium concentration of cluster cations. At a cluster concentration near $5 \times 10^{-4}$ M, the clay becomes saturated and no further binding occurs.

As shown in Figure 1B, the binding of $Ta_6Cl_{12}^{2+}$ to $Na^+$–montmorillonite is similar to the $Nb_6Cl_{12}^{2+,3+}$ system, except that the initial slope of the uptake curve is steeper for $Ta_6Cl_{12}^{2+}$ and the clay becomes saturated at a lower cluster concentration (approximately $1 \times 10^{-4}$ M). It is noteworthy that the binding limit for both $Nb_6Cl_{12}^{2+,3+}$ and $Ta_6Cl_{12}^{2+}$ is 50 ± 2 mmol/100 g. This value is much larger than the maximum loading expected for the exchange of interlayer $Na^+$ by $Nb_6Cl_{12}^{2+,3+}$ or $Ta_6Cl_{12}^{2+}$ (cf., dashed lines in Figure 1).

To better elucidate the binding mechanism, we determined the relationship between the amount of $Na^+$ released to solution and the amount of $Nb_6Cl_{12}^{2+,3+}$ bound. The results are shown in Figure 2. As expected for an ion-exchange mechanism involving displacement of $Na^+$ by $Nb_6Cl_{12}^{2+,3+}$, one observes an initial release of 2.5 equiv of $Na^+$/mol of $Nb_6Cl_{12}^{2+,3+}$. However, as cluster binding continues, the amount of $Na^+$ released per $Nb_6Cl_{12}^{2+,3+}$ decreases. For instance, essentially all of the $Na^+$ has been displaced at a loading of 30 mmol of $Nb_6Cl_{12}^{2+,3+}$/100 g of clay, yet binding of cluster continues up to a limit of 52 mmol/100 g. Thus, there is an apparent decrease in the average cluster charge

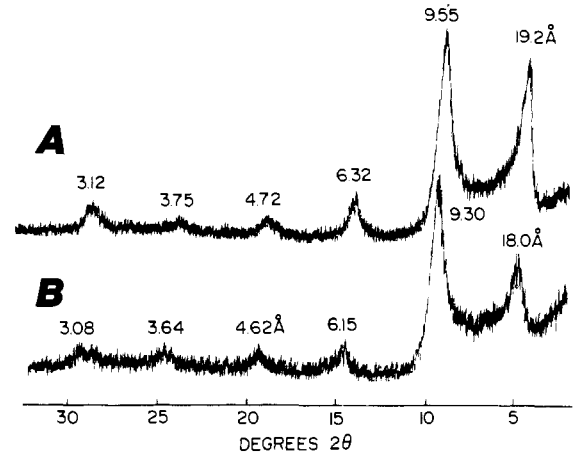


**Figure 3.** 00*l* X-ray reflections for oriented film samples of $Nb_6Cl_{12}^{2+,3+}$–montmorillonite at two cluster loadings: (A) 50.5 mmol/100 g clay, (B) 33.3 mmol/100 g of clay.

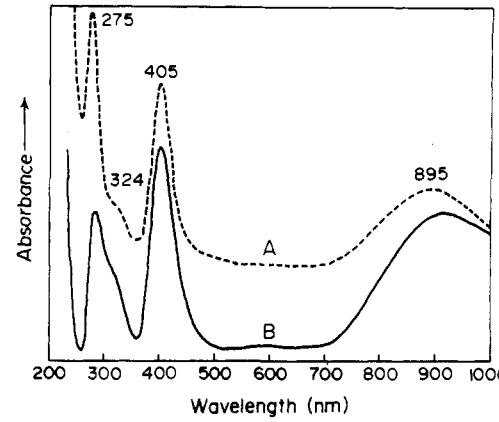


**Figure 4.** UV–Vis spectra: (A) for $Nb_6Cl_{12}^{2+}$ in aqueous solution; (B) for $Nb_6Cl_{12}^{2+}$ intercalated in montmorillonte. The clay sample was in the form of a nujol mull, and the cluster loading was 33 mmol/100 g of clay.

with increasing cluster binding. At the saturation limit, the apparent charge per cluster cation is 1.2+. Curves similar to the one shown in Figure 2 were also observed for the binding of $Nb_6Cl_{12}^{2+}$ and $Ta_6Cl_{12}^{2+}$.

X-ray diffraction patterns of oriented film samples of $Nb_6Cl_{12}^{2+,3+}$, $Nb_6Cl_{12}^{2+}$, and $Ta_6Cl_{12}^{2+}$ indicate that binding occurs on the interlayer surfaces. Figure 3 illustrates the 00*l* reflections for the $Nb_6Cl_{12}^{2+,3+}$ intercalate at two different loadings. The average basal spacings deduced from these reflections are 18.9 ± 0.2 and 18.3 ± 0.2 Å for loadings of 50.5 and 33.0 mmol per 100 g, respectively. Similar values are observed for $Nb_6Cl_{12}^{2+}$– and $Ta_6Cl_{12}^{2+}$–montmorillonite. Under analogous conditions Na–montmorillonite shows only 3 orders of 00*l* reflection and 12.5-Å spacing. Basal spacings of 18.3–18.9 Å are consistent with the van der Waals thickness of a silicate layer and the thickness of an intercalated cluster cation (see below).

UV–vis spectra are shown in Figures 4 and 5, respectively, for $Nb_6Cl_{12}^{2+}$– and $Ta_6Cl_{12}^{2+}$–montmorillonite. Included are spectra for $Nb_6Cl_{12}^{2+}$, $Ta_6Cl_{12}^{2+}$, and $Ta_6Cl_{12}^{3+}$ in aqueous solution. The spectra for $Nb_6Cl_{12}^{2+}$ under homogeneous and intercalated conditions are similar, with the most notable difference being the shift to lower energy of the 895-nm band upon intercalation. The $Nb_6Cl_{12}^{2+}$ ion appears to be relatively stable toward oxidation in the clay interlayers. After 3 days of exposure to the atmosphere, approximately 30% conversion to $Nb_6Cl_{12}^{3+}$ was observed by ESR spectroscopy. In contrast, the intercalation of $Ta_6Cl_{12}^{2+}$ is accompanied by partial oxidation to $Ta_6Cl_{12}^{3+}$, despite attempts to minimize contact with atmospheric oxygen. Thus, the tantalum cluster is much more sensitive to oxidation by atmospheric oxygen in the clay interlayers than in homogeneous solution. The exposure

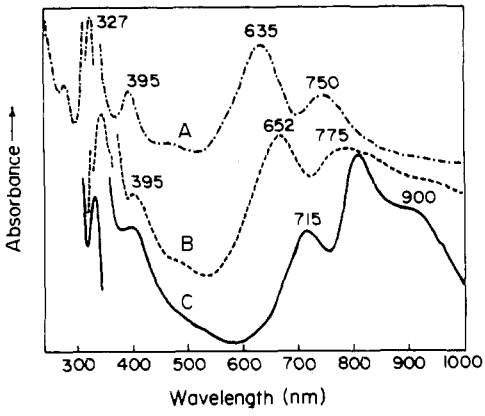


**Figure 5.** UV–Vis spectra: (A) for $Ta_6Cl_{12}^{2+}$ in A aqueous solution; (B) for $Ta_6Cl_{12}^{2+}$ intercalated in montmorillonite. Spectrum C is the solution spectrum of $Ta_6Cl_{12}^{3+}$ formed from $Ta_6Cl_{12}^{2+}$ by oxidation with hydrogen peroxide.

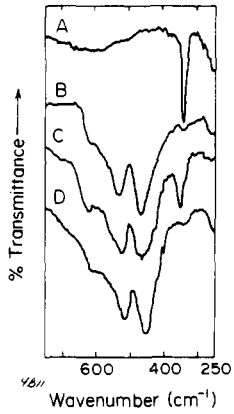


**Figure 6.** Infrared spectra: (A) $[Nb_6Cl_{12}]Cl_2 \cdot 8H_2O$; (B) $Na^+$–montmorillonite; (C) $Nb_6Cl_{12}^{2+}$–montmorillonite (33 mmol/100 g clay); (D) $Nb_6Cl_{12}^{2+}$–montmorillonite that was heated under vacuum at 130 °C for 24 h and at 240 °C for 24 h. All samples were prepared as KBr pellets.

of the desiccated tantalum intercalate to the atmosphere for several hours results in a red-brown product and the appearance of bands at 760, 505, 425, and 353 nm that coresond to the fully oxidized $Ta_6Cl_{12}^{4+}$ cluster.[22]

The infrared spectra of $M_6Cl_{12}^{n+}$–montmorillonites consist essentially of the spectrum of the metal cluster superimposed on that of the clay. Figure 6 illustrates the far-IR spectrum (250–750 $cm^{-1}$) of $Nb_6Cl_{12}^{2+}$–montmorillonite (spectrum C) in comparison to the spectra for $[Nb_6Cl_{12}]Cl_2 \cdot 8H_2O$ (spectrum A) and $Na^+$–montmorillonite (spectrum B). The narrow band at 330 $cm^{-1}$ for $[Nb_6Cl_{12}]Cl_2 \cdot 8H_2O$, assigned previously to a Nb–Cl wagging mode of the cluster core,[23] also is present in the spectrum of the clay intercalate.

The reported hydrolytic instability of $M_6Cl_{12}^{n+}$ cluster cations[13-15,24-25] suggested to us that it may be possible to transform the clusters to small oxide aggregates in the interlayer regions of the clay. Thus, the thermal stability of the intercalates was examined by differential scanning calorimetry (DSC). Figure 7 illustrates the DSC curves for $[Nb_6Cl_{12}]Cl_2 \cdot 8H_2O$ and $Na^+$– and $Nb_6Cl_{12}^{2+}$–montmorillonites. The strong exotherm near 200 °C for the cluster salt has been assigned previously to loss of water coordinated to the metal cluster and within crystallographic cavities.[26] The weaker endotherms above 250 °C result from the loss of HCl and the degradation of the cluster cations.[27]

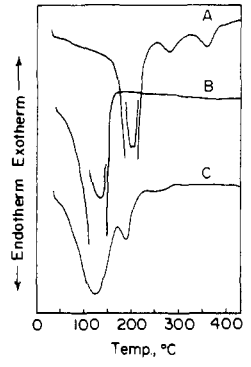


**Figure 7.** DSC curves: (A) $[Nb_6Cl_{12}]Cl_2 \cdot 8H_2O$; (B) $Na^+$–montmorillonite; (C) $Nb_6Cl_{12}^{2+}$–montmorillonite (33 mmol/100 g of clay).

**Table I.** Properties of Intercalates Prepared by the Thermolysis of $Nb_6Cl_{12}^{2+}$- and $Ta_6Cl_{12}^{2+}$-Montmorillonite[a]

| temp, °C | time, h | color | Cl/Nb | $d_{001}$, Å | surf area, $m^2/g$ |
|---|---|---|---|---|---|
| | | A. $Nb_6Cl_{12}^{2+}$-Montmorillonite[a] | | | |
| 25 | | green | | 18.4 ± 0.2 | |
| 130 | 24 | khaki | 1.96 | 19.3 ± 0.6 | 58 |
| 240[c] | 24 | gray | 0.20 | 19.2 ± 0.4 | 64 |
| 325 | 6 | gray | | 18.7 ± 0.6 | 63 |
| 450 | 24 | cream | | 10.0 | |
| | | B. $Ta_6Cl_{12}^{2+}$-Montmorillonite[d] | | | |
| 25 | | blue/green | | 18.3 ± 0.3 | |
| 130 | 24 | blue/green | 2.18 | 18.9 ± 0.3 | |
| 240[e] | 24 | gray | 0.13 | 19.1 ± 0.5 | 32 |
| 350 | 5 | gray | | 19.1 ± 0.4 | 70 |
| 400 | 4 | gray | | 9.7 | |

[a] Samples were prepared by sequential heating under vacuum at the temperatures and for the times indicated. [b] Initial cluster loading was 33 mmol/100 g of clay. [c] Chemical analysis indicated the presence of 1.19 Nb/unit cell. [d] Initial cluster loading was 23 mmol/100 g of clay. [e] Chemical analysis inidcated 0.98 Ta/unit cell.

$Na^+$–montmorillonite exhibits a single endotherm corresponding to loss of interlayer water. Analogous thermal features are found for $Nb_6Cl_{12}^{2+}$–montmorillonite, except that the thermal decomposition of the cluster appears to be initiated at a somewhat lower temperature than for the pure salt.

Although the DSC results indicate that the intercalated cluster cations undergo thermal degradation, all of the intercalates when heated in air above 250 °C exhibit basal spacings of approximately 10 Å. Thus, thermolysis in air apparently results in the migration of metal ions out of the interlayer and the consequent collapse of the silicate layers in van der Waals contact. However, we find that if intercalates containing >20 mmol of $M_6Cl_{12}^{n+}$ per 100 g of clay are heated under vacuum at 130 °C for 24 h followed by 24 h at 240 °C, then stable intercalated products are obtained that contain little or no chlorine.

Table I provides the Cl/M ratios, $d_{001}$ spacings, and $N_2$ BET surface areas for products prepared by thermolysis of $Nb_6Cl_{12}^{2+}$– and $Ta_6Cl_{12}^{2+}$–montmorillonite. Heating the intercalates at 130 °C does not result in the loss of chloride, but subsequent heating to 240 °C eliminates most of the cluster-bound halogen without a significant reduction of the basal spacings. The loss of chlorine from the 240 °C thermolysis product is further indicated by the absence of the Nb–Cl wagging vibration at 330 $cm^{-1}$ (cf., spectrum D in Figure 6). Also, all the UV–vis absorption bands characteristic of $Nb_6Cl_{12}^{2+}$ are lost, and no new bands appear upon thermolysis at 240 °C. It is apparent from these data that the cluster has been oxidized.

Figure 8 illustrates the X-ray diffraction patterns for the products obtained by thermolysis of $Nb_6Cl_{12}^{2+}$–montmorillonite

(22) Espenson, J. H.; McCarley, R. E. *J. Am. Chem. Soc.* **1966**, *88*, 1063.
(23) MacKay, R. A.; Schneider, R. F. *Inorg. Chem.* **1977**, *6*, 549.
(24) Klendworth, P. D.; Walton, R. A. *Inorg. Chem.* **1981**, *20*, 1151.
(25) Field, R. A.; Kepert, D. L. *J. Less-Common Met.* **1977**, *13*, 378.
(26) Schafer, H.; Plautz, B.; Plautz, H. *Z. Anorg. Allg. Chem.* **1976**, *420*, 1.
(27) Spreckelmeyer, B.; Brendel, C.; Dartman, M.; Schafer, H. *Zn. Anorg. Allg. Chem.* **1971**, *386*, 15.
(28) Hahan, R. B. *J. Am. Chem. Soc.* **1951**, *73*, 5091.

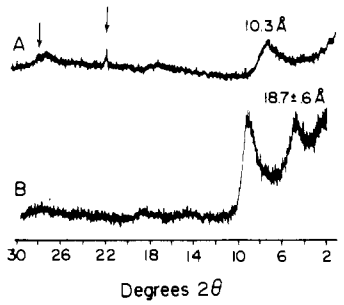


**Figure 8.** X-ray diffraction patterns for $Nb_6Cl_{12}^{2+}$–montmorillonite thermolysis products. Pattern A is for the product obtained by heating the clay under vacuum at 130 °C for 24 h followed by 24 h at 240 °C. Pattern B is for the product obtained by additional heating at 450 °C for 24 h. The arrows indicate the diffraction lines attributed to the formation of a separate $Nb_2O_5$ phase by migration of niobium out of the interlayer region of the clay.

at 240 and 450 °C. The expanded interlayers are retained up to approximately 400 °C, despite the loss of cluster integrity at 240 °C. This observation is explained by the oxidation of the metal to small oxide aggregates comparable in size to an $M_6Cl_{12}^{n+}$ cation. Additional evidence for oxidation in the case of the niobium intercalate is indicated by (i) an increase in the $3d_{5/2}$ binding energy of Nb from 206.5 eV in $Nb_6Cl_{12}^{2+}$–montmorillonite to 208.2 eV in the 240 °C thermolysis product, (ii) the loss of the ESR signal due to trace amounts of $Nb_6Cl_{12}^{3+}$ upon thermolysis at 240 °C, and (iii) the appearance of weak diffraction lines due to $Nb_2O_5$ as a separate phase in the 450 °C thermolysis product (cf., Figure 8).

## Discussion

The binding curves for $Nb_6Cl_{12}^{2+,3+}$ and $Ta_6Cl_{12}^{2+}$, along with the relationship between the $Na^+$ released and $Nb_6Cl_{12}^{2+,3+}$ bound, show that the binding of cluster cation to montmorillonite occurs by the displacement of interlayer $Na^+$. The initial ion-exchange reaction may be written as shown in eq 1, wherein the horizontal

$$M_6Cl_{12}^{n+}(aq) + \overline{nNa^+} \rightleftharpoons \overline{M_6Cl_{12}^{n+}} + nNa^+(aq) \quad (1)$$

lines represent the silicate layers. As the extent of exchange increases, the average charge per cluster decreases. The decrease in cluster charge causes the binding limit to exceed the values expected on the basis of the clay ion-exchange capacity and formal cluster charge.

Anation of the cluster cations by chloride could contribute to a reduction of cluster charge, but such reactions tend to be important in nonaqueous solvents.[23,29] A more plausible explanation is cluster hydrolysis. The structure of these cations consists of an octahedral $M_6$ core with each M–M edge bridged by chlorine. The six equivalent Nb centers are capable of binding various terminal ligands[15,25,29] including water. Thus, the clusters most likely are intercalated initially as $M_6Cl_{12}(H_2O)_6^{n+}$ hydrates that can hydrolyze as shown in eq 2. The position of the hydrolytic

$$\overline{M_6Cl_{12}(H_2O)_6^{n+}} + xH_2O \rightleftharpoons \overline{[M_6Cl_{12}(OH)_x(H_2O)_{6-x}]^{(n-x)+}} + xH_3O^+ \quad (2)$$

equilibrium shifts to the right as cluster loading increases, and the resulting hydrogen ions are displaced by more cluster cations until a complete monolayer of hydrated cations occupies the interlayer surfaces.

The basal spacings of 18.3–18.9 Å for the cluster–clay intercalate are consistent with the van der Waals thickness of a silicate layer (9.6 Å) and a cluster thickness of approximately 9.0 Å. The latter value is in good agreement with the $[M_6Cl_{12}(OH)_x(H_2O)_{6-x}]^{(n-x)+}$ cluster dimension along the $C_3$ axis, as estimated from X-ray crystallographic data[22,30–35] and the van der Waals radius of chlorine (1.8 Å).[36] Thus, the X-ray data indicate that the clusters adopt a preferred interlayer orientation with the $C_3$ axis perpendicular to the silicate sheet. The cluster dimension in the plane perpendicular to the $C_3$ axis is estimated to be approximately 10.4 Å, and if hydrated by one layer of outer-sphere water, approximately 13.0 Å. The observed cluster binding limit of 50 ± 2 mmol/100 g is in reasonable agreement with the expected value (approximately 43 mmol/100 g) for a hydrated monolayer.

The UV–vis and ESR spectroscopic results indicate that intercalated $Nb_6Cl_{12}^{2+}$ is slowly oxidized to $Nb_6Cl_{12}^{3+}$ upon exposure to air over a period of days. In contrast, intercalated $Ta_6Cl_{12}^{2+}$ is readily oxidized to $Ta_6Cl_{12}^{3+}$, and if the amount of interlayer water is reduced by desiccation, complete oxidation to $Ta_6Cl_{12}^{4+}$ can be observed. Tantalum clusters are known to be more easily oxidized than the niobium analogues even in aqueous solution.[15]

An early investigation[13] of $Nb_6Cl_{12}^{2+}$ hydrolysis under basic conditions suggested the formation of cluster cations containing $\mu$-hydroxo ligands. A more recent study[14] of niobium and tantalum bromide clusters showed that the cluster integrity was lost under basic conditions. Reaction 3 was proposed to explain the sudden decrease in pH that accompanied the loss of cluster structure.

$$[M_6Br_8(OH)_4](OH)_6^{4-} + 5H_2O \rightleftharpoons 3M_2O_5 + 4H^+ + 8Br^- + 8H_2 \quad (3)$$

We propose an analogous oxidation by water to explain the conversion of intercalated cluster cations to metal oxide clusters upon thermolysis under vacuum at 240 °C. For the case of $Nb_6Cl_{12}^{2+}$–montmorillonite, where the average charge per partially hydrolyzed cluster is near 1+, the reaction may be written as shown in eq 4.

$$\overline{Nb_6Cl_{12}(OH)(H_2O)_5^+ + 9H_2O} \xrightarrow{240\ °C} \overline{3Nb_2O_5 + H^+} + 12HCl(g) + 8H_2(g) \quad (4)$$

The role of the 130 °C pretreatment, which is essential for restricting migration of cluster cations out of the interlayer at elevated temperatures, is uncertain. One possibility is that the pretreatment influences the extent of cluster hydrolysis and/or limits the amount of interlayer water to the most tightly bound water in the first hydration sphere of the cluster, thus restricting the mobility of the cluster. However, further studies of this point are needed.

Relatively little is known at this point concerning the structure of the intercalated oxide aggregates, except that the apparent size of the aggregate is approximately 9.0 Å in the direction perpendicular to the silicate layers. A 9.0-Å lattice expansion is compatible with the presence of three to four planes of oxygen atoms in the interlayer. Although molecular oxides such as $M_6O_{15}$ have not been observed previously, related hexanuclear oxoanions of the type $M_6O_{19}^{8-}$ exist.[37,38] It is plausible that $M_6O_{15}$ aggregates or higher oligomers constructed from such aggregates are stabilized on the intracrystal surfaces of the clay. Regardless of the precise structure of the intercalated oxide aggregates, the presence of 1–1.2 interlayer metal ions per unit cell leads to porous structures with surface areas (32–70 $m^2/g$) that are appreciably larger than $Na^+$–montomirllonite (10–15 $m^2/g$).

The $M_6Cl_{12}^{n+}$ cluster cations themselves also function as pillars as evidenced by the 58 $m^2/g$ surface area for $Nb_6Cl_{12}^{2+}$–montmorillonite at 130 °C and a cluster loading of 33 mmol/100 g (cf., Table I). At the loading limit of 50 ± 2 mmol/100 g (1.8 Nb/cell), the interlayers are effectively "stuffed" with complex

(29) MacKay, R. A.; Schneider, R. F. *Inorg. Chem.* **1968**, *7*, 455.
(30) Thaxton, C. B.; Jacobson, R. A. *Inorg. Chem.* **1971**, *10*, 1460.
(31) Semon, A.; Schnering, H. G.; Wohrle, H.; Schafer, H. *Z. Anorg. Allg. Chem.* **1965**, *339*, 155.
(32) Simon, A.; Schnering, H. G.; Schafer, H. *Z. Anorg. Allg. Chem.* **1968**, *361*, 235.
(33) Koknat, F. W.; McCarley, R. E. *Inorg. Chem.* **1972**, *11*, 1812.
(34) Vaughan, P. A.; Sturdivant, J. H.; Pauling L. *J. Am. Chem. Soc.* **1950**, *72*, 5477.
(35) Converse, J. G.; McCarley, R. E. *Inorg. Chem.* **1970**, *9*, 1361.
(36) Bondi, A. *J. Phys. Chem.* **1964**, *68*, 441.
(37) Nelson, W. H.; Tobias, R. S. *Inorg. Chem.* **1963**, *2*, 985.
(38) Nelson, W. H.; Tobias, R. S. *Can. J. Chem.* **1964**, *42*, 731.

cations and low surface areas are expected. However, at a loading of 33 mmol/100 g a $N_2$ BET surface area of approximately 180 $m^2/g$ is expected, provided the clusters are uniformly distributed through the interlayers. Thus, the observed value of 58 $m^2/g$ is only about one-third the value expected on the basis of cluster loading and size. This suggests that the clusters may tend to concentrate near the edges of certain interlayers and restrict access to those interlayers. Spatial redistribution of cluster cations within an interlayer can also lead to interstratification of collapsed and stuffed interlayers. Some degree of interstratification is suggested, in fact, by the asymmetry of the 001 and 002 X-ray reflections in Figure 3B. Nonuniformity in the cluster cation distribution, of course, will also result in interstratification and decreased surface areas for the thermolysis products containing metal oxide pillars.

## Conclusion

This work demonstrates for the first time that metal cluster cations can be intercalated by an ion-exchange mechanism in a typical smectite clay and oxidized in situ to metal oxide aggregates that function as molecular size pillars. The intercalation chemistry for the particular niobium and tantalum clusters selected for study is complicated in part by hydrolysis, air oxidation, cluster migration, and nonuniform cluster distributions. Nevertheless, the synthetic approach may prove to be generally useful for the preparation of clays pillared by metal oxides that do not have stable polyoxycation precursors in aqueous solution.

**Acknowledgment.** The partial support of this work by the National Science Foundation through Grant No. 83-06583 is gratefully acknowledged. S.P.C. thanks the Dow Chemical Co. for a summer research fellowship, and J.W. thanks the Ministry of Education of the People's Republic of China for a scholarship. We also thank Dr. Luis Matienzo of Martin-Marietta Corp. for providing us with the XPS data, and B. Martin for assistance in obtaining the chemical analyses.

---

Contribution from the Institut für Anorganische und Analytische Chemie, Freie Universität Berlin, 1000 Berlin 33, West Germany, and Institut für Physikalische und Theoretische Chemie, Universität Tübingen, 7400 Tübingen, West Germany

# Pentafluoroselenium Cyanate, $F_5Se—O—C\equiv N$

K. SEPPELT* and H. OBERHAMMER

*Received August 1, 1984*

The previously described pentafluoroselenium isocyanate, $F_5Se—N=C=O$, has been demonstrated to be $F_5Se—O—C\equiv N$, according to electron diffraction, $^{77}Se$ and $^{14,15}N$ NMR, and vibrational spectroscopy. The other possible isomers, the nitrile oxide, $F_5Se—C\equiv N—O$, and the fulminate, $F_5Se—O—N\equiv C$, are excluded by means of geometrical and chemical reasons, respectively.

## Introduction

Pentafluorosulfur isocyanate, $F_5S—N=C=O$,[1] and its tellurium analogue, $F_5Te—N=C=O$,[2] are best prepared from the corresponding amines $F_5SNH_2$ and $F_5TeNH_2$[4] and carbonyl halides. So, there was never any doubt about their isocyanate structure, and a recent electron diffraction work gave practically identical geometric parameters for the isocyanate parts in both molecules.[5] See also Table I.

$F_5SeNH_2$ does not exist. For the preparation of $F_5Se—N=C=O$ two reactions were tried that worked successfully in the preparation of $F_5Te—N=C=O$,[6] namely

$$Hg(OTeF_5)_2 + 2ClCN \rightarrow HgCl_2 + F_5Te—N=C=O$$

$$Xe(OTeF_5)_2 + HCN \rightarrow Xe + HOTeF_5 + F_5Te—N=C=O$$

Only the second reaction was successful in the case of the selenium system. The resulting material had the expected melting point, boiling point, mass spectrum, and IR absorption band at 2290 $cm^{-1}$, so we assumed that $F_5Se—N=C=O$ had been prepared. The electron diffraction structure on this material resulted in reasonable NC and CO distances. The SeNC angle, however, turned out to be almost 10° smaller than the corresponding angle in $F_5SNCO$ and $F_5TeNCO$ (Table I).

There were other doubts about the isocyanate nature of the novel material. There is a strong IR absorption at 1104 $cm^{-1}$, which was assigned to $\nu_s(N=C=O)$, but in $F_5S—N=C=O$ and $F_5Te—N=C=O$ this is very weak, as expected. Also, the selenium material was the only one that was exploive when pure. And despite many attempts, not a single chemical reaction occurred that was typical of an isocyanate.[6] With $F_5SNCO$ and $F_5TeNCO$ such reactions could well be performed.[6,7] In light of these results, we reviewed the electron diffraction and IR data and also measured $^{125}Te$, $^{77}Se$, $^{33}S$, $^{14}N$, and $^{15}N$ NMR spectra of these three materials.

## Experimental Section

Pentafluorosulfur isocyanate and pentafluorotellurium isocyanate were prepared according to literature methods[1,2] from $F_5SNH_2$ and $F_5TeNH_2$. Pentafluoroselenium cyanate was prepared from $Xe(OSeF_5)_2$ and HCN, as described in ref 6. The electron diffraction data of Oberhammer et al.[5] were used in this analysis.

NMR spectra were taken on a JEOL FX90Q instrument equipped with a multinuclear probehead and operated at a frequency of 89.55 MHz for protons. Experimental conditions (10-mm sample diameter): $^{19}F$, 84.25 MHz, 29-μs pulse width for a 90° pulse, 1–10 scans, no delay time between pulses on top of the acquisition time; $^{125}Te$, 18.25 MHz, 36-μs pulse width, 1000–10000 scans, no further pulse delay, as above; $^{77}Se$, 17.03 MHz, 17-μs pulse width, 10 000–20 000 scans, no further pulse delay, as above; $^{33}S$, 6.83 MHz, 20-μs pulse, 100 000 scans, no further pulse delay; $^{15}N$, 9.03 MHz, 26-μs pulse width, 1000scans, 100-s pulse delay; $^{14}N$, 6.43 MHz, 37-μs pulse width, 2000 scans, no further delay.

The chemical shifts were measured externally against the standards $C^{19}FCl_3$ (neat), $^{125}Te(OH)_6/H_2O$, $^{77}SeOCl_2$ (neat), $(NH_4^+)_2{}^{33}SO_4^{2-}/H_2O$, and $^{14,15}NH_4{}^{+14,15}NO_3^-/H_2O$.

## Results and Discussion

For a complete survey we took all possible isomers $F_5SeXYZ$ into consideration: $F_5Se—N=C=O$, the isocyanate; $F_5Se—O—C\equiv N$, the cyanate; $F_5Se—O—N\equiv C$, the fulminate; $F_5Se—C\equiv N—O$, the nitrile oxide.

The original electron diffraction data were used to determine the skeletal geometric parameters for all four isomers.[5] The details

* To whom correspondence should be addressed at the Freie Universität Berlin.

(1) Duncan, L. C.; Rhyne, T. C.; Clifford, A. F.; Shaddix, R. E.; Thompson, J. W. *J. Inorg. Nucl. Chem. Suppl.* **1967**, 33.
(2) Hartl, H.; Huppmann, P.; Lentz, D.; Seppelt, K. *Inorg. Chem.* **1983**, *22*, 2183.
(3) Clifford, A. F.; Duncan, L. C. *Inorg. Chem.* **1966**, *5*, 692.
(4) Seppelt, K. *Inorg. Chem.* **1973**, *12*, 2837.
(5) Oberhammer, H.; Seppelt, K.; Mews, R. *J. Mol. Struct.* **1983**, *101*, 325.
(6) Huppmann, P.; Klöter, G.; Thrasher, J. S.; Seppelt, K.; DesMarteau, D. D. *Inorg. Chem.* **1984**, *23*, 2217.
(7) Thrasher, J. S.; Howell, J. L.; Clifford, A. F. *Inorg. Chem.* **1982**, *21*, 1616.

0020-1669/85/1324-1227$01.50/0 © 1985 American Chemical Society